NANO EXPRESS

Evolution of wetting layer in InAs/GaAs quantum dot system

Y. H. Chen · X. L. Ye · Z. G. Wang

Abstract For InAs/GaAs quantum dot system, the evolution of the wetting layer (WL) with the InAs deposition thickness has been studied by reflectance difference spectroscopy (RDS). Two transitions related to the heavy- and light-hole in the WL have been distinguished in RD spectra. Taking into account the strain and segregation effects, a model has been presented to deduce the InAs amount in the WL and the segregation coefficient of the indium atoms from the transition energies of heavy- and light-holes. The variation of the InAs amount in the WL and the segregation coefficient are found to rely closely on the growth modes. In addition, the huge dots also exhibits a strong effect on the evolution of the WL. The observed linear dependence of In segregation coefficient upon the InAs amount in the WL demonstrates that the segregation is enhanced by the strain in the WL.

Keywords Quantum dots · Wetting layer · Reflectance difference spectroscopy · Segregation

PACS 78.67.Hc · 68.65.Hb · 73.21.Fg

A strained epilayer with a thickness beyond a critical value will change from layer-by-layer growth (Frank–van der Merwe growth) to island growth (Stranski–Krastanow growth) in order to relax strain energy. When covered by barrier materials, these self-assem-

Y. H. Chen (✉) · X. L. Ye · Z. G. Wang
Key Laboratory of Semiconductor Materials Science,
Institute of Semiconductors, Chinese Academy of Sciences,
P.O. Box 912, Beijing 100083, P.R. China
e-mail: yhchen@red.semi.ac.cn

bled nanometer-scale islands become the so-called quantum dots (QDs), which have attracted much attention due to the interest in their fundamental physics and potential application in novel devices [1]. The optical and electrical properties of the self-assembled QDs can be affected greatly by the wetting layer (WL) around the dots [2–5]. The WLs serve as channels for carriers to fall into dots and to redistribute between the dots, strongly influencing on the emission properties of the dots [2, 3]. It was also predicted that the WLs could limit greatly the modulation response of QD lasers [4]. Therefore the information of electronic states and structures of WLs is desirable for understanding the properties of the QDs and their devices. However, unlike QDs, which can be characterized straightly by atomic force microscopy (AFM), transmission electron microscopy (TEM) and photoluminescence (PL), etc. [1], it is quite difficult to access experimentally the information of WLs. Occasionally WLs can be observed in PL excitation and photoreflectance (PR) measurements [6]. The direct observation has been achieved by the cross-sectional STM measurements under an ultra-high vacuum environment [7, 8]. However, there is still no systematical experiment research on the evolution of WLs up to now.

In this letter, reflectance difference spectroscopy (RDS) will be adopted to characterize the WL in the InAs/GaAs system. RDS is a sensitive tool for characterizing the in-plane optical anisotropy (OA) of surfaces and quantum wells (QWs), in which the symmetries are reduced due to the surface reconstruction and the inversion asymmetry of the QWs, respectively [9, 10]. OA is expected for an InAs WL, which behaves as an asymmetric InGaAs QW due to

the segregation effect [11]. The transition energies of WLs can be obtained from the RD spectra, which offers a method to study WLs. By pausing substrate rotation, non-homogeneous InAs deposition can be realized on a GaAs surface [12], which enables us to study the WL of various deposition thickness that are grown under the same growth conditions.

The samples are prepared on a 2-in. semi-insulating GaAs substrate in a Riber-32p MBE system under an As$_2$ flux of 5×10^{-6} Torr. After the growth of 100 nm-GaAs buffer layer at 580 °C, the growth temperature was reduced to 530 °C and another 2 nm-GaAs was grown. Then an InAs layer of averaged 2 ML was deposited at a rate of 0.008 ML/s. Afterwards, 5 nm-GaAs, 100 nm-GaAs, and 2 nm-GaAs were grown at 530 °C, 580 °C, and 530 °C, respectively. Finally another 2 ML InAs layer was grown for the AFM measurements. After growth of each InAs layer a growth interruption of 2 min was introduced to allow a full diffusion of indium atoms on the surface. Note that the substrate stops rotating during the InAs deposition in order to achieve the expected non-homogeneous InAs distribution [12]. In this case, the incidence angle of the indium beam is about 35 °, and the distance between the indium source and the sample is about 10 cm. After growth the wafer was cut into 16 pieces with a size of about 3 mm along the direction where the InAs thickness varies gradually. The 16 pieces were numbered from 1 for the thinnest to 16 for the thickest. An almost linear variation of InAs amount with the samples can be predicted on the basis of the cosine law for the MBE source beam [13]. The relative reflectance difference between the [110] and [1$\underline{1}$0] directions,

$\rho = 2(r_{110} - r_{1\underline{1}0})/(r_{110} + r_{1\underline{1}0})$, was measured for all samples by the RDS at room temperature. The RDS setup has been given in our previous work [10].

The samples are first characterized by AFM in contact mode. Figure 1a shows the typical surface morphology of six samples. The structural parameters of InAs QDs obtained from AFM results have been summarized in Fig. 1(b, c). No QD in samples 1–3 simply reflects a FM growth of the InAs layer. For the samples 4 and 5, a few InAs QDs appear in the surface, indicating a growth transition from FM into SK mode. For the samples 6–12, the dot density increases quickly and saturates at a level of about 8×10^9/cm^2, while the averaged height keeps almost unchanged. When the InAs thickness is further increased in the samples 13–16, the averaged height drops apparently from 12 nm to 8 nm, and the lateral size increases from 42 nm to 53 nm, indicating a ripening process [14]. In samples 9–16, some huge InAs dots are found with the sizes two times or more larger than that of the around dots. It is generally believed that the huge dots tend to relax strain energy via the generation of dislocations, which in turn enhances their ability to capture the indium atoms. The density of the huge dots is also plotted in Fig. 1b. Clearly they prefer to be formed at the initial stage of the dot formation (samples 5 and 6) or under thicker InAs depositions (samples 9–16). In contrast to the rich information about the InAs dots, no information can be obtained for the WL from the AFM measurements.

Figure 2a shows RD spectrum (ρ) and its second derivative spectrum with respect to wavelength ($d^2\rho/d\lambda^2$) of the sample 10. In RD spectrum three features at

Fig. 1 (a) AFM images (2 μm × 2 μm) of the samples 2, 4, 6, 8, 10 and 12. Different gray-scales are adopted in the images. Arrows point out the huge dots, which may be incoherent to the GaAs. (b and c) Density of InAs dots N_{QD} (squares), density of huge InAs dots N_{LQD} (circles), averaged height (squares) and base area (circles) of InAs dots obtained from AFM results. FM, SK and R denote the Frank–van der Merwe, Stranski–Krastanow and ripening growth modes, respectively
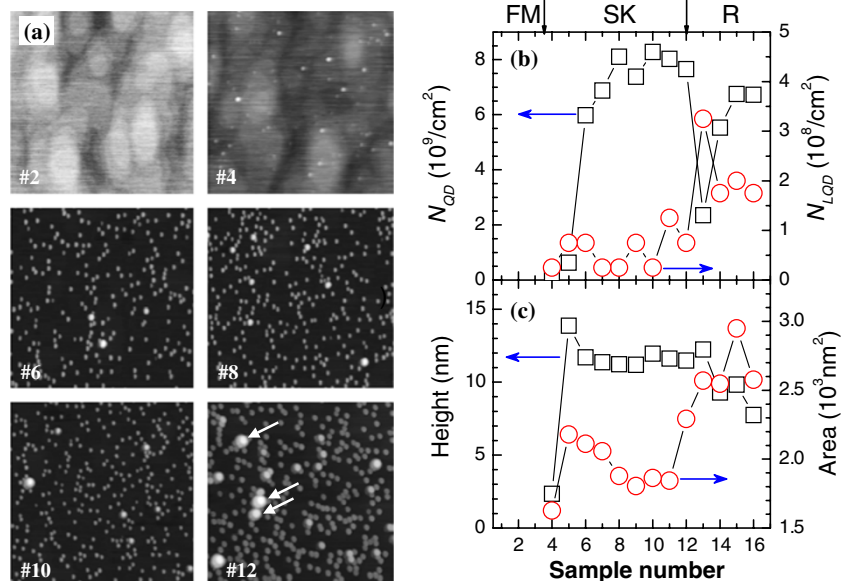
Fig. 2 (**a**) RD spectrum (ρ) and its second derivative spectrum with respect to wavelength ($d^2\rho/d\lambda^2$) of the sample 10. The GaAs band edge, LH- and HH-hole related transitions in the WL are indicated by the arrows. Inset shows the sample structure. (**b**)Variation of $d^2\rho/d\lambda^2$ spectrum with the samples indicated by the color contrast. The wavelengths of the three transitions are indicated by triangles, squares and circles, respectively
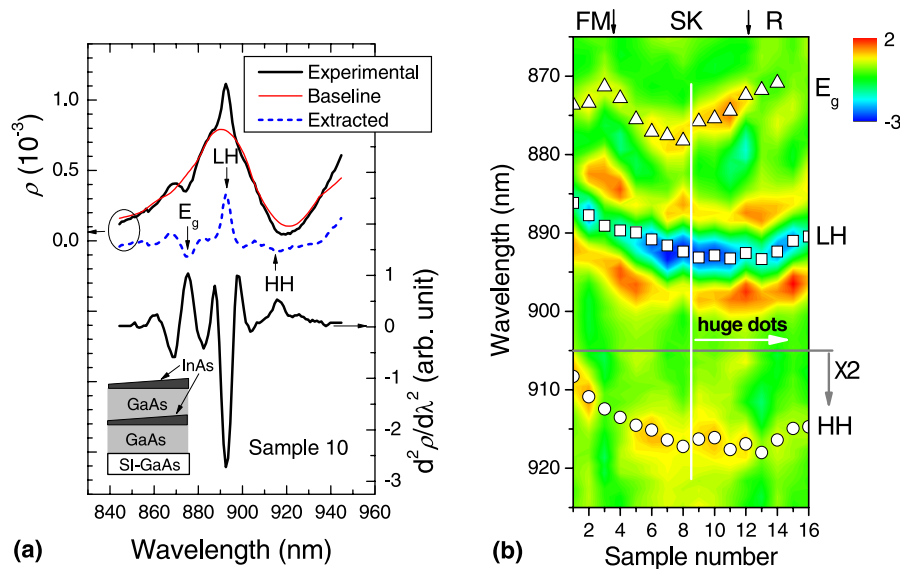
875.4 nm, 892.8 nm, and 916.1 nm, superimposed over a broad structure (baseline) shown as a thin curve, are assigned to the transitions related to GaAs band edge, the LH and HH transitions in the buried WL, respectively. At present it is not clear where the broad structure comes from. Three structures are even clear in the extracted RD spectrum and $d^2\rho/d\lambda^2$ spectrum. Note that the surface WL has no bound state due to the narrow well width and the extremely high barrier of the vacuum. Because of the heavier effective mass of the HH, the HH transition energy is very sensitive to the fluctuation in composition and thickness of the WL, that is why the HH structure is broadened. Figure 2b shows the $d^2\rho/d\lambda^2$ spectrum varying with the samples. The wavelength shifts of the GaAs, LH and HH features are clearly indicated by the triangles, squares, and circles, respectively.

The OA reflects a symmetry reduction of the WL, which arises probably from segregation effect and lateral compositional modulation (LCM) in the WL [10, 15]. It is well known that the indium atoms will segregate to surface during the capping process, leading to an asymmetric InGaAs QW with a width of several nanometers [11]. On the other hand, the InGaAs stripes or elongated structures along the [1$\bar{1}$0] direction were frequently observed for InAs deposited on the GaAs surface [16, 17]. This LCM structures can be preserved after the capping process and cause an anisotropic strain in the WL. The variation of the OA of the WL shown in Fig. 2(b) therefore implies a systematical change of the segregation or LCM in the WL. The detailed discussion is beyond the scope of this letter.

The shift of the LH and HH structures shown in Fig. 2b reveals the variation of the total InAs amount in the WL. We have presented a calculation model to calculate the transition energies related to the HH and LH holes in the WL. The model takes into account not only the strain effect, and different effective masses for InAs and GaAs, but also the segregation effect of indium atoms. Due to the segregation effect, the buried InAs WL can be treated as an asymmetric quantum well with an exponentially decayed composition distribution, i.e., the distribution of indium atoms in WL (X_{In}) can be given by

$$X_{In} = \begin{cases} 0 & z<0 \\ \frac{t_{WL}}{l}\exp(-z/l) & z>0 \end{cases}, \quad (1)$$

where $z = 0$ is the position where InAs is deposited, t_{WL} is the InAs amount in the WL, l is the segregation length of the indium atoms. The segregation coefficient R is related to the segregation length via $R = \exp(-a_c/2l)$ with a_c of the lattice constant of GaAs. In principle the unknown t_{WL} and R can be determined from the HH and LH transition energies uniquely, if the HH and LH exciton binding energies (E_{hh}^{ex} and E_{lh}^{ex}) are known. The two reference samples with InAs deposition thickness of 1 ML and 1.7 ML have been adopted for the calibration of E_{hh}^{ex} and E_{lh}^{ex}. For the 1.7 ML sample, the QDs are formed at 1.6 ML monitored by RHEED, i.e., $t_{WL} = 1.6$ ML. Assumed $E_{hh}^{ex} = cE_{lh}^{ex}$ with c independent upon t_{WL} ($c = 1.4$ in our calculations), the unkown parameter E_{hh}^{ex} for $t_{WL} = 1$ ML and 1.6 ML can be determined uniquely from the reference samples. Then E_{hh}^{ex} for t_{WL} between 1 ML and 1.6 ML can be further obtained via the linear interpolation, which is $E_{hh}^{ex} = 19.83t_{WL} - 12.13$ (meV) in our calculations. With the calibrated E_{hh}^{ex} and E_{lh}^{ex}, it is straight to fit the

HH and LH transition energies by t_{WL} and R. The details of the calculations will be given elsewhere.

The deduced t_{WL} and R are shown in Fig. 3. During the FM growth (samples 1–3), the deposited InAs is only distributed in the WL, leading to a linear increase of t_{WL}. During the SK growth, t_{WL} still increases linearly but at a slower rate for samples 4–8. However, for samples 9–12, t_{WL} stops increasing probably due to the formation of the huge InAs dots. The dislocated InAs dots can serve as the sink centers for indium atoms, therefore reduce the growth rate of the WL effectively. When the ripening process occurs, t_{WL} is actually reduced, indicating that not only the newly deposited InAs but also the part of WL are absorbed by the InAs islands. From Fig. 3, it is found the InAs islands start to appear when t_{WL} is larger than 1.3 ML. This value is apparently less than 1.5–1.7 ML, which is usually regarded as the critical thickness for InAs dot to form on GaAs [18]. This can be attributed to the desorption of indium atoms due to the high growth temperature (530 °C) and the slow growth rate.

Since the samples are grown at a very slow rate and relatively higher temperature, we can adopt an equilibrium model presented by Daruka and Barabási to discuss the above results [14]. According to the model, t_{WL} increases linearly with the InAs deposition thickness within the FM growth regime, and then the growth rate of WL becomes slower during the SK growth due to the competition of the InAs dots. Finally t_{WL} saturates at a maximum value when the ripening occurs. The theoretical results can explain partly the result in Fig. 3, i.e., the evolution of t_{WL} for samples 1–8. However, for samples 9–16 the experimental data deviate from the prediction of the model apparently. It is probably due to the huge dots that are formed in samples 9–16. As stated early, these huge dots can relax their strain via the generation of dislocations, therefore their ability to absorb the indium atoms is greatly enhanced. This suggestion consists with the increase of the density of the huge dots in samples 9–16.

The obtained R shows a variation very similar to that of t_{WL} as shown in Fig. 3. This suggests that the formation and ripening of the islands play also an important role in the segregation effect. The inset in Fig. 3 shows R versus t_{WL}, where a linear relation between R and t_{WL} is observed. Clearly it reflects a simple fact that the segregation is enhanced greatly by the strain in the WL. It is worth to point that R is in the range of 0.8–0.87 after the dots are formed. These values agree well with the reported data determined by other methods, for examples, R is estimated about 0.79 in Ref. [19], and in the range of 0.85–0.87 in Ref. [20].

The resonant structure in vicinity of 875 nm in Fig. 2b comes from the GaAs strained by the deposited InAs. At present we cannot distinguish whether it come from the GaAs beneath the surface InAs layer or the region associated to the buried InAs layer. The N-like shift of the energy with the InAs deposition indicates an interesting evolution of the strain in the GaAs around the InAs layers. The further research is needed to clarify the details.

In summary, the HH and LH related transitions of the InAs WL have been observed in RD spectra, from which the InAs amount in the WL and the In segregation coefficient are determined. The transitions between FM, SK, and R growth modes have been revealed clearly by the variation of the InAs amount in the WL and the In segregation coefficient. In addition, the formation of dislocated dots is also suggested to affect greatly the evolution of the WL. The linear dependence between In segregation coefficient and the InAs amount in the WL reflects that the segregation is enhanced by the strain in WL.
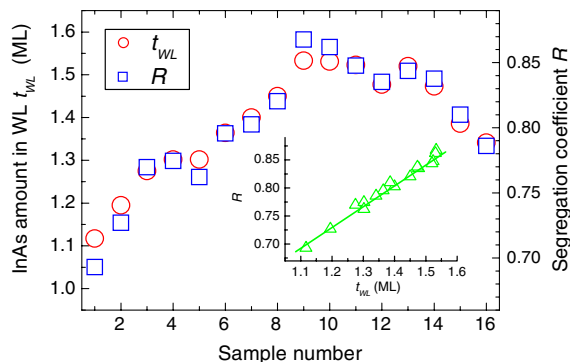
Fig. 3 The deduced InAs amount in the WL t_{WL} (circles) and the segregation coefficient R (squares) for the 16 samples. Inset shows the segregation coefficient versus the InAs amount in WL

References

1. D. Bimberg, M. Grundmann, N.N. Ledentsov, *Quantum dot heterostructures*, (John Wiley & Sons Ltd., Chichester, 1999)
2. S. Sanguinetti, M. Henini, M. Grassi Alessi et al., Phys. Rev. B **60**, 8276 (1999); S. Sanguinetti, T. Mano, M. Oshima et al., Appl. Phys. Lett. **81**, 3067 (2002)
3. Y. Toda, O. Moriwaki, M. Nishioka, Y. Arakawa, Phys. Rev. Lett. **82**, 4114 (1999)
4. D.G. Deppe, D.L. Huffaker, Appl. Phys. Lett. **77**, 3325 (2000)
5. R.V.N. Melnik, M. Willatzen, Nanotechnology **15**, 1 (2004)
6. W. Rudno-RudziÒski, G. SJk, K. Ryczko et al., Appl. Phys. Lett. **86**, 101904 (2005)
7. B. Shin, B. Lita, R.S. Goldman, J.D. Phillips, P.K. Bhattacharya, Appl. Phys. Lett. **81**, 1423 (2002)

8. P. Offermans, P.M. Koenraad, J.H. Wolter, K. Pierz, M. Roy, P.A. Maksym, Physica E **26**, 236 (2005)

9. Z. Sobiesierskiy, D.I. Westwood, C.C. Matthai, J. Phys. Condens. Matter **10**, 1 (1998)

10. Y.H. Chen, X.L. Ye, J.Z. Wang, Z.G. Wang, Z. Yang, Phys. Rev. B **66**, 195321 (2002); X. Ye, Y.H. Chen, B. Xu, Z.G. Wang, Mater. Sci. Eng. B **91–92**, 62 (2002)

11. A. Rosenauer, D. Gerthsen, D. Van Dyck et al., Phys. Rev. B **64**, 245334 (2001)

12. M.J. da Silva, A.A. Quivy, P.P. González-Borrero, E. Marega Jr., J. Cryst. Growth **236**, 41 (2002)

13. M.A. Herman, H. Sitter, *Molecular beam epitaxy: fundamental and current status*, (Springer-Verlag, Berlin, Heidelberg, 1989), p. 32

14. I. Daruka, A. Barabási, Phys. Rev. Lett. **79**, 3708 (1997)

15. F.A. Zhao, Y.H. Chen, X.L. Ye et al., J. Phys. Condens. Matter **16**, 7603 (2004)

16. R. Heitz, T.R. Ramachandran, A. Kalburge et al., Phys. Rev. Lett. **78**, 4071 (1997)

17. T.J. Krzyzewski, P.B. Joyce, G.R. Bell, T.S. Jones, Surf. Sci. **517**, 8 (2002)

18. F. Patella, S. Nufris, F. Arciprete, M. Fanfoni, E. Placidi, A. Sgarlata, A. Balzarotti, Phys. Rev. B **67**, 205308 (2003)

19. P. Offermans, P.M. Koenraad, J.H. Wolter, K. Pierz, M. Roy, P.A. Maksym, Physica E **26**, 236 (2005)

20. P. Offermans, P.M. Koenraad, R. Nötzel, J.H. Wolter, K. Pierz, Appl. Phys. Lett. **87**, 111903 (2005)